Hindawi
Adsorption Science & Technology
Volume 2021, Article ID 5545683, 11 pages
https://doi.org/10.1155/2021/5545683

Research Article

Adsorptive Removal of Malachite Green Dye onto Coal-Associated Soil and Conditions Optimization

T. R. Sundararaman,[1] **A. Saravanan**,[1] **P. Senthil Kumar**,[2,3] **M. Millicent Mabel**,[1] **R. V. Hemavathy**,[1] **S. Karishma**,[1] **S. Jeevanantham**,[1] **R. Hemavathi**,[1] **A. Ishwariya**,[1] **and S. Kowsalya**[1]

[1]*Department of Biotechnology, Rajalakshmi Engineering College, 602105, Chennai, India*
[2]*Department of Chemical Engineering, Sri Sivasubramaniya Nadar College of Engineering, 603110, Chennai, India*
[3]*Centre of Excellence in Water Research (CEWAR), Sri Sivasubramaniya Nadar College of Engineering, 603110, Chennai, India*

Correspondence should be addressed to P. Senthil Kumar; senthilkumarp@ssn.edu.in

Received 28 February 2021; Revised 10 May 2021; Accepted 12 June 2021; Published 28 June 2021

Academic Editor: Monoj Kumar Mondal

The present research was investigated to eliminate the cationic dye (malachite green (MG)) from the water environment using coal-associated soil. The adsorbent material was characterized using scanning electron microscopy (SEM) and Fourier Transform Infrared Spectrophotometer (FTIR) analyses. Batch experiments were performed to investigate the different factors which affect the adsorption study. The maximum percentage removal of MG dye was attained as follows: adsorbent dose of 1.0 g/L (0.2 to 1.6 g/L), solution pH of 6.0 (2.0 to 9.0), temperature of 30°C (30 to 60°C), time contact of 60min (10 to 90 min), and dye's concentration of 25 mg/L (25 to 150 mg/L). The adsorption isotherm was studied with four different isotherm models and results showed that the Freundlich isotherm model gave the best fit than the other nonlinear models to designate the isotherm behaviours with R^2 value of 0.9568, and the maximum adsorption capacity of coal-associated soil for MG dye adsorption is 89.97 mg/g. The evaluation of kinetic studies was performed by using three different kinetic models, where it exposed that pseudofirst order providing the best fit with R^2 value of 0.96 (25 to 150 mg/L). The thermodynamic parameters Gibbs free energy (ΔG°), entropy (ΔS°), and enthalpy (ΔH°) were endorsing that the present adsorption system was exothermic. Thus, the experimental results state that coal-associated soil could be an alternative material for the exclusion of dyes from water.

1. Introduction

In the current era, water scarcity is one of the environmental issues prevailing in the world. With an expanding population, industrialization, and less availability of freshwater resources, the demand for clean water has increased worldwide [1, 2]. Availability of clean water is required for both industrial purposes and household activities. Release of industrial effluents and prolonged excessive use of fertilizers and pesticides in agricultural fields causes deterioration in the water quality resulting in water contamination or pollution [3, 4]. In most industries, without proper treatment, effluents are discharged into water resources. Industrial effluents can be remediated to remove hazardous chemicals which can further be utilized for industrial or other activities [5–7]. Hence, wastewater treatment has gained significant attention in recent years. Dyes are one such chemical occurring in industrial discharges [8–10]. The occurrence of lesser concentrations of toxic dyes in water has a consequential impact on the environment. Dyes are mostly discharged from textile, food, pharmaceutical, paper, printing, leather, and cosmetic industries [11–13]. Of these, textile industries contribute to most of the dye pollution. Owing to the inefficacy of dye molecules for complete attachment onto fabrics, the majority of the dyes are released into the environment [14–16]. Dye effluents discharged from industries have received remarkable attention owing to the effects caused by it. A large number of hazardous chemicals are present in dye effluents expelled from

industries. These chemicals pollute water and cause harmful effects on the aquatic environment [17–19]. Human health is also affected by these harmful chemicals. The release of toxic amines due to the decomposition of dyes can cause serious health impacts on animals and humans. Besides, the process of photosynthesis is also influenced by dye color, preventing the penetration of light. Environmental health is also deteriorated by the occurrence of dye molecules [20–23].

Various types of synthetic dyes are produced and employed for industrial purposes annually. MG dye is such an organic cationic basic dye. MG dye is widely employed in the textile, leather, and paper industries. Other applications of MG dye include usage as fungicide and parasiticide in aquaculture field, food additive or food coloring agent, and as an anthelminthic [24, 25]. However, several studies are reporting the hazardous and toxic effects of MG dye. The strong metal ions chelating tendency of MG dyes increases its toxicity towards aquatic organisms. Plant roots absorb water along with the dye molecules presents it which affects the metabolic process of the plants. Untreated MG dye molecules could enter and accumulate in the food chain causing teratological, mutagenic, and carcinogenic threats to mammalian cells. Other health effects include the liver, spleen, heart damage, skin lesions, and reduction in fertility rates, food intake, and growth. Despite this, they also act as a tumor promoter in liver cells by reducing leucomalachite green, increasing its persistence, and inducing apoptosis and tumor. Thus, there is prime importance in the removal or treatment of MG dye effluent due to its toxic impacts on the ecosystem [26–28].

Flocculation, coagulation, ultrasonication, rhizoremediation, membrane filtration, precipitation, adsorption, electrochemical oxidation, ozonation, reverse osmosis, and phytoremediation are some of the familiar techniques used for the elimination of dyes [29–31]. However, some of the negative aspects such as high operation cost, generation of byproducts, and poor removal of the complex organic structure have paved the way for researchers to shift their attention towards an adsorption process of wastewater treatment [32, 33]. A nonreactive, equilibrium process that involves in particle accumulation at the two-phase interface is known as adsorption [34]. Being cost-effective, simple operation, and highly efficient, adsorption strategy is widely used for the elimination of toxic dyes from the contaminated environment [35–37]. Also, the performance of adsorptive separation improves with the characteristics of the adsorbent [38]. Properties such as functional group, surface area, nontoxicity, reusability, and cost of the adsorbent are of paramount importance in the dye expulsion from industrial effluents [39, 40]. Different adsorbents exploited for MG dye adsorption include nylon microplastics [41], almond gum [42], litchi peel biochar [43], calcium alginate nanoparticles [44], Avenasativa hull [45], brewer's spent grain [46], nanocomposites [47], and clayey soil [48]. In some cases, the expensiveness of activated carbon prepared from various materials limits its usage in the dye removal process. Hence, few studies have been carried out with soil as an adsorbent, for example, surface soils [49] and Laterite soil [50]. Coal-associated soil usually comprises few mineral-carrying oxides such as silicon dioxide (SiO_2), manganese dioxide (MnO_2), and aluminium oxide (Al_2O_3). These oxides have active sites and carbon present in the coal has mesoporous components which have the efficacy to adsorb dye molecules from industrial or aqueous effluents. Along with the mineral oxides, a sufficient quantity of carbon is also present in the coal-associated soil [51]. The advantages of using coal-associated soil involve the effective physical properties and characteristic features of the pore structure improvement mechanism. It also enhances mass transfer operation which is observed between the adsorbate and the adsorbents.

The present study focuses on utilizing coal-associated soil as adsorbents for MG dye removal from synthetic solutions. The characterization studies such as FTIR and SEM analysis were performed to analyze the surface property of adsorbent material. Batch adsorption study of different parameters—-concentration of adsorbate, equilibrium time, best adsorption pH, temperature, and coal-associated soil dosage—was carried out to optimize the variables. Four distinct isothermal adsorption models and three different kinetic models were examined to extract information regarding the adsorption mechanism and kinetic rate of MG dye onto coal-associated soil. The thermodynamic analysis was studied to predict the nature of the adsorption process (exothermic or endothermic).

2. Experimental

2.1. Adsorbate. Malachite Green (MG) dye, 0.1 M HCL, and 0.1 N NaOH were purchased from E Merck (India) Pvt. Ltd. MG dye standard solution was arranged by liquefying 1 g of MG dye in 1 L of refined water. Dilution of the standard solution with distilled water was carried out to acquire requisite concentrations of dye solution (25 mg/L to 150 mg/L). Adjustment of pH solution was made by using 0.1 Molar HCl/0.1 Molar NaOH. The concentration of dye in the solution (before and after adsorption) was determined by ultraviolet-visible spectroscopy.

2.2. Adsorbent Preparation and Characterization. Coal-associated soil was collected from the Mannargudi coalfield, Tamil Nadu, India. To eliminate dust particles, the soil was rinsed with water and allowed for drying at room temperature. The dried soil samples were sieved through a mesh sieve to acquire the desired adsorbent for the MG dye removal. The qualitative analysis of coal-associated soil before and after adsorption was performed using FTIR and SEM analysis.

2.3. Batch Experimental Studies. A batch study was performed to investigate the factors affecting variables. Studies were conducted in an Erlenmeyer flask of 250 mL capacity comprising desired adsorbent measure with a notable concentration of MG dye solution. For a known contact time, the solution mixture was left to undergo agitation in a temperature-controlled shaking incubator. After definite time interims, centrifugation was carried out to separate adsorbate and soil adsorbent. The final concentration of MG dye was deliberated using ultraviolet-visible spectroscopy. MG removal was examined using the following equation.

$$\%\text{removal} = \frac{(C_i - C_f)}{C_i} \text{x}100, \quad (1)$$

where C_i and C_f indicate the initial concentration and final concentration of MG dye (mg/L).

2.4. Thermodynamic Analysis. Thermodynamic studies were carried out by carrying out the adsorption process at different temperatures (303 K to 333 K) in an incubation shaker. At a prearranged phase interims, samples were centrifuged and the remaining concentration of dye in the solution was analyzed using ultraviolet-visible spectroscopy. Thermodynamic parameters were evaluated using the following equation.

$$K_c = \frac{C_{Ae}}{C_e}, \quad (2)$$

$$\Delta G^\circ = -\text{RTlnK}_c, \quad (3)$$

$$\text{LogK}_c = \frac{\Delta S^\circ}{2.303\text{R}} - \frac{\Delta \text{H}^\circ}{2.303\,\text{R}\,\text{T}}, \quad (4)$$

where C_{Ae} represents the quantity of adsorbate adsorbed onto coal-associated soil per liter of the solution (mg/L), C_e represents the measure of the concentration of adsorbate in the equilibrium solution, K_c represents the equilibrium constant, and T represents the temperature of the solution (K).

2.5. Study of Adsorption Isotherm and Kinetics. Adsorption isotherm studies were executed at different adsorbate concentrations (25 mg/L to 150 mg/L) by defining other experimental variables as constant. The equilibrium adsorption capacity of the coal-associated soil was assessed by the following formula.

$$q_e = \frac{(C_i - C_f)V}{m}, \quad (5)$$

where q_e represents adsorption capacity at equilibrium, V represents solution volume of MG dye, and m represents the mass of coal-associated soil adsorbent. The acquired equilibrium data was studied into four distinct adsorption isothermal models—Langmuir, Freundlich, Kahn, and RadkePrausnitz. Nonlinear regression investigation was performed by MATLAB R2016a to determine different factors such as error values—sum of squared error (SSE), root mean squared error (RMSE), and correlation coefficient (R^2).

Kinetic studies were performed by agitating flasks comprising different concentrations of dye solutions (25 mg/L to 150 mg/L) and the required amount of adsorbent at different time intervals (10 min to 90 min). At a prearranged time, the samples were introverted, centrifuged, and analyzed in ultraviolet-visible spectroscopy. Removal of MG dye onto coal-associated soil at distinct time interims is evaluated by the following equation.

$$q_t = \frac{(C_o - C_t)V}{m}, \quad (6)$$

where q_t represents the quantity of adsorbate adsorbed onto coal-associated soil at any time t (mg/g) and C_o and C_t represent the concentration of MG dye solution initially and at a specific time t (mg/L). By using the MATLAB R2016a software, nonlinear regression analysis was performed, and kinetic model parameters—R^2, SSE, and RMSE—were calculated.

3. Results and Discussion

3.1. Adsorbent Characterization-SEM and FTIR. The surface structure and porous nature of the adsorbent were studied using SEM analysis. Figures 1(a) and 1(b) depict the SEM analysis of coal-associated soil before and after the adsorption of MG dye. Rough permeable structure with higher craters can be perceived in SEM analysis of coal-associated soil before adsorption in Figure 1(a). It also illustrates the presence of increased surface area with irregular and interconnected pores for the efficient adsorption of MG dye molecules. Figure 1(b) displays the formation of the agglomerate after the adsorption of MG dye. Thus, the disappeared pores with a smooth surface and agglomerates confirm the MG dye adsorption onto coal-associated soil.

FTIR analysis of coal-associated soil before and after adsorption of MG dye was analyzed. Peaks at 3400.63 cm^{-1} and 3420.95 cm^{-1} indicate the occurrence of NH-stretching and hydrogen-bonded OH groups. Before adsorption, an intense peak at 2848.85 cm^{-1} confirms C-H stretching in alkanes. The occurrence of other functional groups such as aromatic ring stretching, aliphatic fluoro compounds, and aliphatic and aromatic phosphate compounds is established by the absorption mounts at 1613.90 cm^{-1}, 1114.42 cm^{-1}, 1009.91 cm^{-1}, and 910.99 cm^{-1}. The sharp intense peak at 1032.58 cm^{-1} relates to the silicone group and primary amine (C-N) broadening [52]. From the FTIR analysis of coal-associated soil before adsorption, it can be inferred that alcohol and amine groups could form covalent bond-forming a matrix structure facilitating the removal of MG dye molecules. Broad absorption peaks 1419.81 cm^{-1} and 1123.94 cm^{-1} in after adsorption denotes the vinyl C-H group, organic sulfates, and sulfate ions. Peaks at 1525.52 cm^{-1} and 1061.52 cm^{-1} signifies the N-O asymmetric stretching in nitro compounds and aliphatic amines. This result after adsorption confirms the coal-associated soil has greater adsorption capability.

3.2. Impact of Coal-Associated Soil Dose. The effect of coal-associated soil dose on MG dye removal was deliberated by changing the dosage (0.2 to 1.6 g/L) and keeping other factors constant. Figure 2 displays the influence of adsorbent dose on the removal of MG dye molecules. The graph reveals that the adsorbate removal improves with the upsurge in the dosage of soil adsorbent up to 1 g/L. The availability of more locates on the soil surface is the cause for the enhanced removal. With advanced raise in adsorbent dose, MG dye removal persisted constantly due to low driving force and saturation of active sites on the surface of the soil adsorbent [52]. An optimum amount of coal-associated soil for the adsorption of MG dye was found to be 1 g/L.

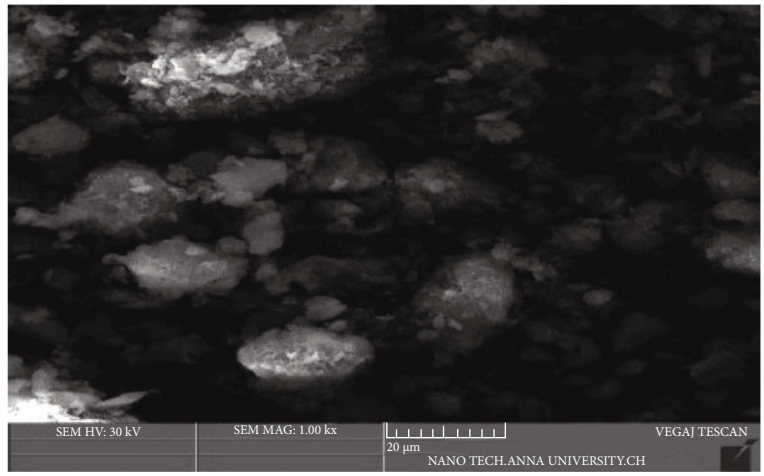

(a)

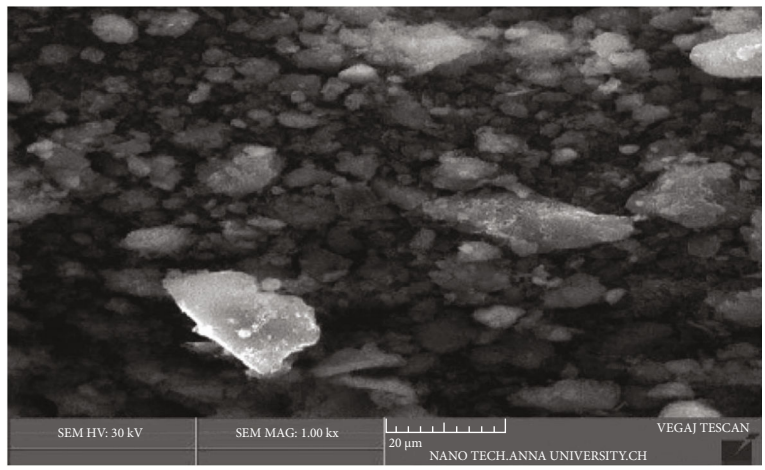

(b)

Figure 1: (a) SEM analysis of coal-associated soil (before adsorption). (b) SEM analysis of coal-associated soil (after adsorption).

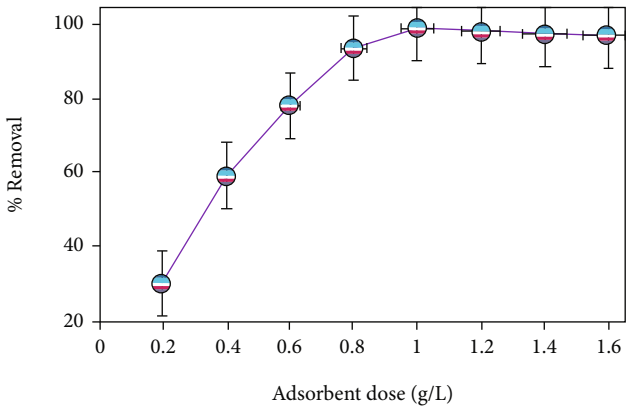

Figure 2: Impact of the adsorbent dosage on the adsorption of MG dye onto coal-associated soil.

3.3. Impact of Temperature. Batch adsorption studies were performed at diverse temperatures (303, 313, 323, and 333 K) and different dye concentrations (25–150 mg/L). Figure 3(a) shows the effect of temperature on the adsorption of MG dye onto coal-associated soil. It can be perceived from Figure 3(a) that MG dye removal declined with raise in temperature due to the weak adsorptive forces between MG dye molecules and adsorbent surface resulted in reduced removal of MG dye from the synthetic solution. This indicates that adsorption was exothermic and the optimal temperature for the MG dye removal was experimental to be 30°C.

3.4. Thermodynamic Analysis. The thermodynamic investigation was studied to understand the randomness, spontaneity, and exothermic or endothermic nature of MG dye adsorption onto coal-associated soil. Figure 3(b) demonstrates the graph of log K_c vs. 1/T, the values of ΔS° and ΔH° were calculated from the graph. Thermodynamic factors such as ΔG°, ΔS°, and ΔH° were shown in Table 1. The decrease in negative values of ΔG° with an increase in concentration was observed. Moreover, negative ΔS° values indicate the decreased randomness of the adsorbed MG dye molecules. From the negative values of ΔG°, ΔS°, and ΔH°, it is concluded the adsorption process was random, impulsive, and exothermic [53].

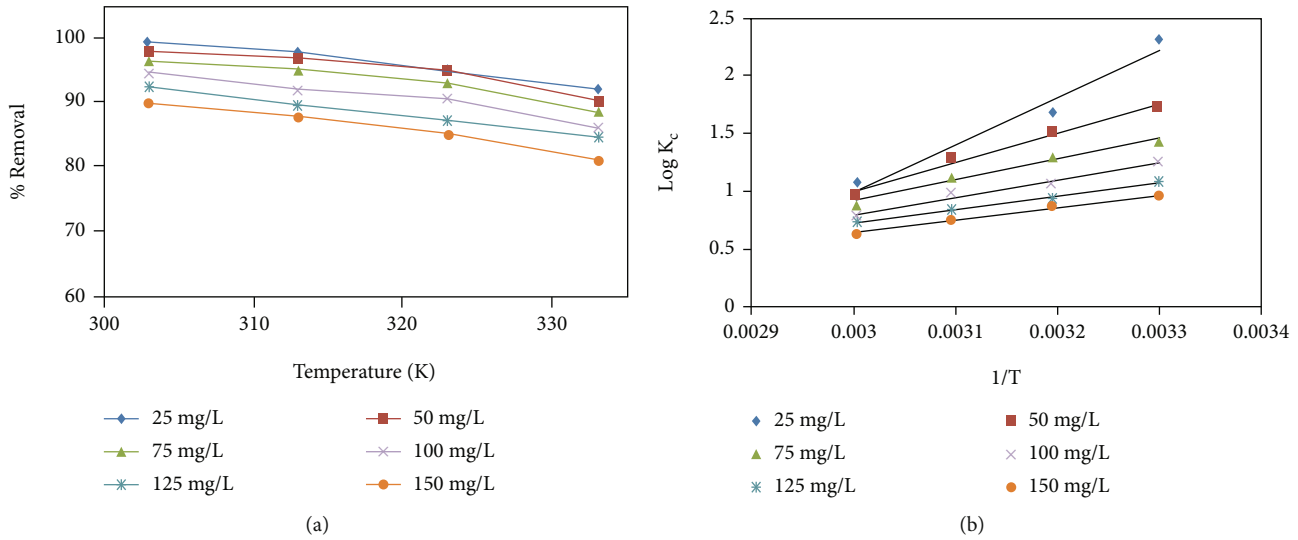

Figure 3: (a) Impact of temperature for the elimination of MG dye onto coal-associated soil. (b) Thermodynamic analysis for the removal of MG dye on coal-associated soil.

Table 1: Thermodynamic factors for the elimination of MG dye on coal-associated soil.

C_o (mg/L)	ΔS° (J mol^{-1})	ΔH° (kJ mol^{-1})	ΔG° (kJ mol^{-1})			
			30°C	40°C	50°C	60°C
25	-221	-80	-13	-10	-8	-7
50	-122	-47	-10	-9	-8	-6
75	-88	-35	-8	-8	-7	-6
100	-70	-29	-7	-6	-6	-5
125	-53	-22	-6	-6	-5	-5
150	-50	-21	-6	-5	-4	-4

3.5. Impact of pH. Batch adsorption experimentations were performed with diverse solution pH varying from 2.0 to 9.0 by fixing other factors constant. Figure 4 depicts the impact of pH for the MG dye removal onto coal-associated soil. It revealed that the adsorption of MG dye was augmented with a pH value of 2.0 to 6.0. Due to electrostatic repulsion at the acidic conditions, slow removal was observed. Ionization of carboxyl functional groups might have resulted in a sudden enhancement in dye removal percentage. The maximal removal was observed at pH 6.0. Owing to deprotonation of amine groups beyond the pH value of 6.0, equilibrium adsorption condition is attained and the removal gradually decreases. Thus, the optimal pH for the adsorption onto coal-associated soil was identified to be pH 6.0.

3.6. Impact of Interactive Time. A batch study was performed with varying interactive time intervals of 10 min to 90 min. Figure 5(a) displays the impact of interactive time studies. Due to high dynamic locates on the surface of coal-associated soil, enhanced interaction of MG dye molecules was detected at the initial stage of adsorption which is revealed from Figure 5(a). As time proceeds, attainment of equilibrium of active sites resulted in reduced removal of MG dye molecules. Moreover, as the contact time increases,

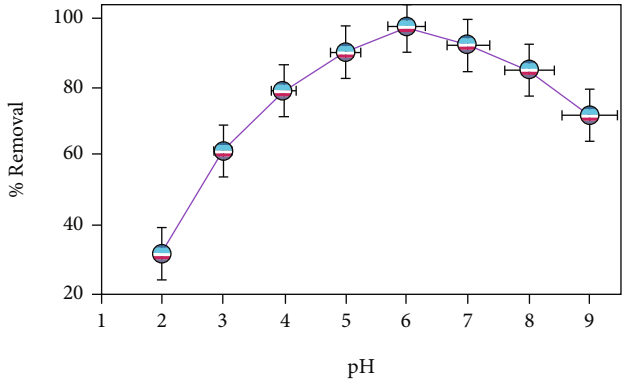

Figure 4: Impact of pH for the elimination of MG dye onto coal-associated soil.

dye molecules aggregate making it unfeasible for diffusion. Thus, the higher percentage removal of MG dye onto coal-associated soil was observed with the contact time of 60 min.

3.7. Adsorption Kinetic Study. In the real-time application, sorption kinetics plays a crucial role in describing the rate-controlling steps, mechanism, and mass transfer. The data from the interactive study were fitted using three adsorption kinetic models (pseudofirst-order kinetics, pseudosecond-order kinetics, and Elovich kinetics). The following mathematical relationships were employed to represent the adsorption kinetic models.

Pseudofirst order [54]:

$$q_t = q_e(1 - \exp(-k_1 t)). \tag{7}$$

Pseudosecond order [55]:

$$q_t = \frac{(q_e^2 k_2 t)}{(1 + q_e k_2 t)}. \tag{8}$$

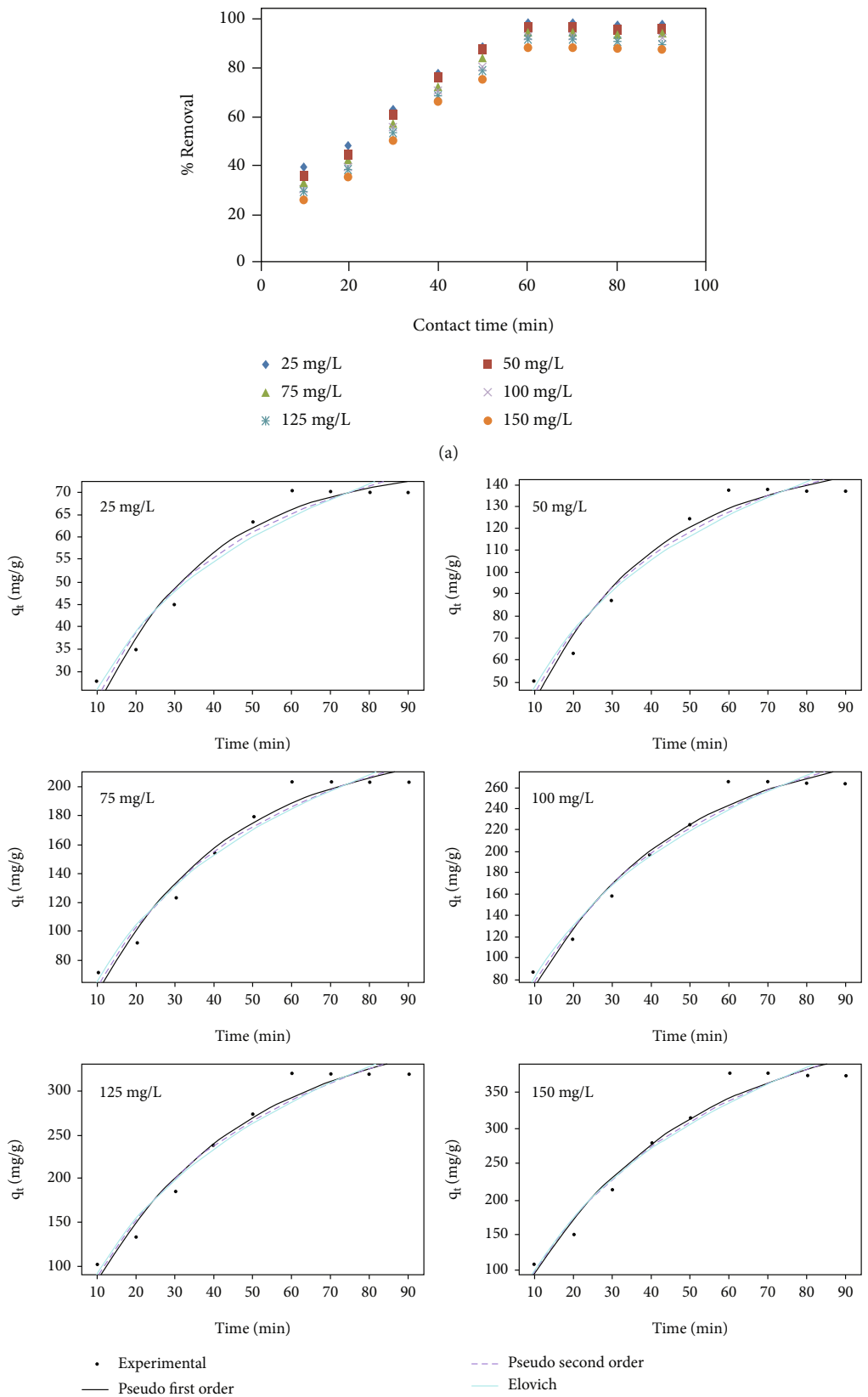

Figure 5: (a) Impact of interactive time for the elimination of MG dye on coal-associated soil. (b) Adsorption kinetic modeling study for the elimination of MG dye on coal-associated soil.

Table 2: Adsorption kinetic factors for the elimination of MG dye on coal-associated soil.

C_o (mg/L)	q_e (exp)	Pseudofirst order			Pseudosecond order			Elovich		
		q_e (mg/g)	k_1 (min^{-1})	R^2	q_e (mg/g)	k_2 (g/mg min)	R^2	α_E (mg/g min)	β_E (g/mg)	R^2
25	73.08	75.81	0.0342	0.9627	99.56	0.0003	0.9594	0.0138	11.08	0.9531
50	140.85	151.2	0.0319	0.9657	202.7	0.0001	0.9579	0.005	24.67	0.9488
75	205.66	228.2	0.0292	0.967	311.8	0.0001	0.961	0.0025	39.92	0.9541
100	266.17	302	0.0273	0.971	419.5	0.0004	0.9654	0.0016	55.78	0.9592
125	319.98	369.7	0.0261	0.9671	520.1	0.0002	0.9604	0.0011	70.96	0.9536
150	375.11	446.1	0.0243	0.9675	641.3	0.0001	0.96	0.0007	91.21	0.9526

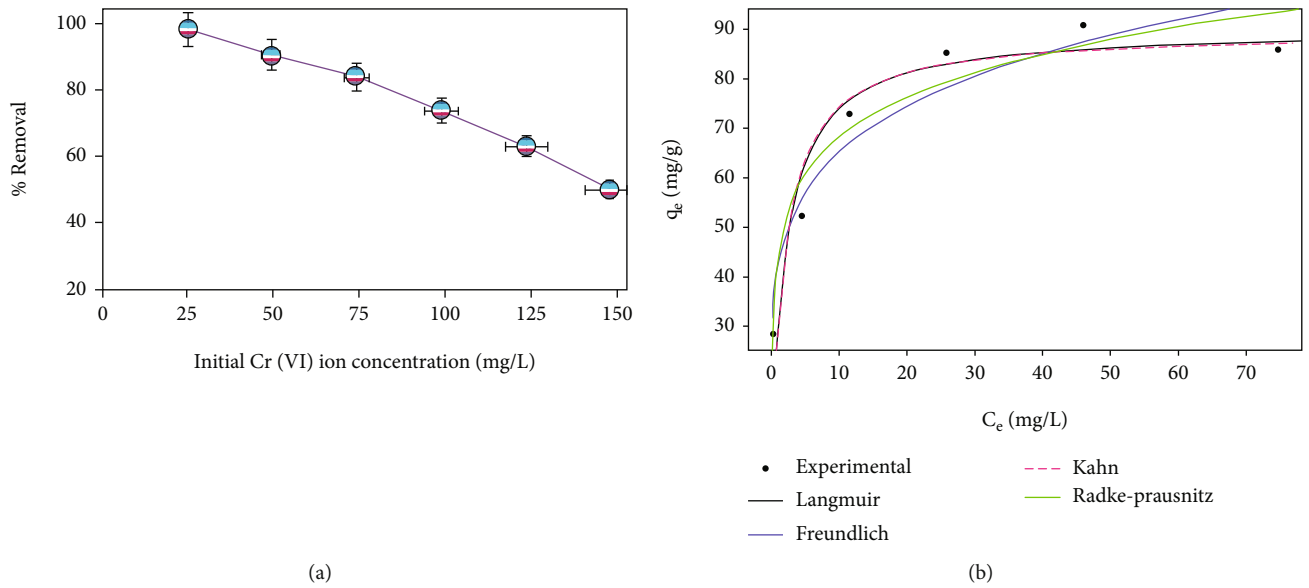

Figure 6: (a) Impact of dye's initial concentration on the adsorption of MG dye onto coal-associated soil. (b) Adsorption isothermal study for the elimination of MG dye on coal-associated soil.

Elovich kinetic [56]:

$$q_t = (1 + \beta_e) \ln (1 + a_E \beta_E t), \quad (9)$$

where k_1 and k_2 represent the pseudofirst-order rate constant (min^{-1}) and pseudosecond-order rate constant (g mg^{-1} min^{-1}), α_E represents the initial adsorption rate (mg/g/min), and β_E desorption constant (g/mg).

From the plot of adsorption kinetic data q_e vs. t, values of kinetic constants, SSE and RMSE, and R^2 values were calculated and listed in Table 2. Adsorption kinetic fit for adsorption of MG dye on coal-associated soil was depicted in Figure 5(b). From Table 2, it can be observed that with the escalation in dye concentration, rate constant values decline which indicates less competition for dye molecules at the active locates of soil adsorbent at low concentrations. As the dye concentration increases, there will be complex opposition for dynamic locations subsequently occasioning lesser adsorption rates. Chemical adsorption on a highly heterogeneous surface is explained by Elovich kinetic model. But due to low R^2 values, the Elovich kinetic model is not suited to denote the absence of chemisorption. The higher R^2 values of pseudofirst-order kinetic were found to be best fitted for the present adsorption system.

3.8. Impact of Adsorbate Concentration. The impact of the initial concentration of MG dye in the current adsorption system is portrayed in Figure 6(a). Studies were performed with diverse adsorbate concentrations (25, 20, 75, 100, 125, 150 mg/L) with an adsorbent dosage of 1 g/L and pH of 6.0. From Figure 6(a), it can be observed that adsorption of MG dye declines with raise in adsorbate concentration. The reason behind this is at a low concentration of dye, soil adsorbent has adequate active sites on its surface facilitating its adsorption. But at high concentrations, the adsorbent surface is deficient in free active sites resulting in reduced dye removal [40]. The maximum removal of MG dye was perceived at 25 mg/L.

3.9. Adsorption Isotherm Study. The isothermal study helps to recognize the adsorption mechanism of the interface between MG dye and coal-associated soil [57]. In the present analysis, Langmuir, Freundlich, Kahn, and Radke-Prausniiz model has been employed to examine the MG dye adsorption onto coal-associated soil. Figure 6(b) displays the isothermal

Table 3: Adsorption isotherm factors for MG dye adsorption onto coal-associated soil.

S. no.	Isotherm model	Parameters	Correlation coefficient (R^2)	Errors	
				SSE	RMSE
1	Langmuir	$q_m = 89.97$ (mg/g) $K_L = 0.461$ (L/mg)	0.864	40.7	10.09
2	Freundlich	$K_F = 41.85\left((\text{mg/g})\,(\text{L/mg})^{(1/n)}\right)$ $n = 5.205$ (g/L)	0.9568	21.9	5.399
3	Kahn	$q_m = 8.189$ (mg/g) $a_K = 0.091$ $b_K = 0.461$	0.864	41.9	11.65
4	RadkePrausnitz	$q_{\text{mRP}} = 38.53$ (mg/g) $K_{\text{RP}} = 5.252$ mRP = 0.8515	0.9075	157.2	7.238

study of MG dye adsorption onto coal-associated soil and the data were listed in Table 3.

3.9.1. Langmuir Isotherm. Theoretically, Langmuir adsorption isotherm is based on a few assumptions—maximal adsorption, while the adsorbent surface is occupied with saturated monolayer solute molecules, absence of adsorbate migration at the surface plane. Nonlinear Langmuir isotherm is expressed as follows [58]:

$$q_e = \frac{q_m K_L C_e}{1 + K_L C_e}, \tag{10}$$

where q_m denotes the monolayer adsorption capacity at equilibrium (mg/g) and K_L is the Langmuir energy constant. From the plot of q_e vs. C_e correlation coefficient $R^2 = 0.864$, q_m and K_L are 89.97 mg/g and 0.461 L/mg, respectively.

3.9.2. Freundlich Isotherm. Freundlich isotherm model applies to heterogeneous exteriors. It also suggests that with the completion of active centers on the adsorbent surface, an exponential decrease in adsorption energy can be noticed. Freundlich isotherm equation is represented as follows [59]:

$$q_e = K_F C_e^{\frac{1}{n}}, \tag{11}$$

where K_F is the Freundlich constant describing adsorption coefficient (L/g) and n is the Freundlich exponent denoting the deviation measure from adsorption linearity. $1/n$ represents the heterogeneity factor. From Table 3, it can be perceived that the value of $n = 5.205$ g/L indicated the physical adsorption process. And also, higher correlation coefficient value ($R^2 = 0.9568$) signifies the best fitting nature of the adsorption model.

3.9.3. Kahn Isotherm. Temperature independence of adsorption potential is signified by the Kahn isotherm model. It implies that the dependence of the adsorption process on adsorbent and adsorbate nature. Kahn isotherm equation is given as follows [60]:

$$q_e = \frac{q_{\max} b_k C_e}{(1 + b_k C_e) a_k}, \tag{12}$$

where a_k is the exponent value of Kahn isotherm and b_k signifies the Kahn isotherm constant.

3.9.4. Radke-Prausnitz Isotherm. For a wide range of adsorbent concentrations, Radke-Prausnitz isotherm is identified to be more suitable. Radke-Prausnitz isotherm equation can be described as follows [61]:

$$q_e = \frac{q_{\text{mRP}} K_{\text{RP}} C_e}{(1 + K_{\text{RP}} C_e)^{\text{MRP}}}, \tag{13}$$

where q_{MRP} represents the adsorption capacity of Radke-Prausnitz (mg/g). From the study, Radke-Prausnitz's

Table 4: Monolayer adsorption capacity of different adsorbents for the elimination of MG dye.

S. no.	Adsorbent	q_m (mg/g)	References
1	Conch shell powder	92.3	[62]
2	Coal associated soil	89.97	Present study
3	Coconut AC	83.06	[63]
4	*Limoniaacidissima* shell	80.64	[64]
5	Rice husk	76.92	[65]
6	*Prosopis cineraria* saw dust	65.8	[66]
7	Nylon microplastics	63.48	[41]
8	Rattan sawdust	62.71	[67]
9	Oxalic acid modified mice husk	54.02	[68]
10	Pine needles	52.91	[69]
11	*Borassusaethiopum* flower	48.23	[70]
12	Alg-Fe_3O_4 nanoparticles	47.84	[71]
13	Citric acid-treated pea shells	14.49	[72]
14	Commercial AC	8.27	[73]
15	CPAC/chitosan composite	4.8	[74]

maximum adsorption capacity was elucidated to be 38.53 mg/g. Based on high R^2 values and SSE and RMSE, the experimental data yielded adsorption isotherm results in the following order: Freundlich > RadkePrausnitz > Langmuir > Kahn isotherm model. From the higher correlation coefficient value $R^2 = 0.9568$, it can be confirmed that Freundlich isotherm was best fitted which specifies the multilayer removal of MG dye on coal-associated soil and the heterogenic nature of the adsorbent surface. Performance comparison of estimated q_m value of the present adsorption system with distinct adsorbents used for MG dye removal is summarised in Table 4. The results represent that the monolayer adsorption capacity of coal-associated soil was identified as higher when it was compared with other adsorbents, because coal-associated soil has mineral-carrying oxides which have active sites to enhance the adsorption process.

4. Conclusion

Coal-associated soil used in the study is abundantly, freely available and is anticipated to be economical for the exclusion of MG dye. The qualitative analysis such as SEM and FTIR was performed for the coal-associated soil adsorbent, and the results corroborated the presence of adequate characteristics such as cavities, pores, and essential functional groups for MG dye removal from polluted water. The different essential parameters for MG dye removal were optimized via batch adsorption study as adsorbent dosage—1.0 g/L, temperature—30°C, pH—6.0, interactive time—60 min, and initial MG dye concentration—25 mg/L. Freundlich isotherm suited well with the experimental results explaining the multilayer adsorption of MG dye onto coal-associated soil. The maximum adsorption capacity of coal-associated soil was found to be 89.97 mg/g. In terms of kinetics, pseudofirst order was the best fitting model revealing the physical nature of the MG dye adsorption process. The exothermic, feasible, and spontaneous nature of the adsorption process was confirmed from the thermodynamic results. Therefore, the present study infers the potentiality of coal-associated soil as a desirable and economically feasible adsorbent for the removal of toxic dyes from the wastewater.

Data Availability

Data available on request from the authors.

Conflicts of Interest

The authors declare that they have no conflicts of interest.

References

[1] H. Sharifpour, N. Javid, and M. Malakootian, "Investigation of single-walled carbon nanotubes in removal of Penicillin G (Benzyl penicillin sodium) from aqueous environments," *Desalination and Water Treatment*, vol. 124, pp. 248–255, 2018.

[2] N. Javid, Z. Honarmandrad, and M. Malakootian, "Ciprofloxacin removal from aqueous solutions by ozonation with calcium peroxide," *Desalination and Water Treatment*, vol. 174, pp. 178–185, 2020.

[3] A. H. Mahvi, M. Malakootian, and M. R. Heidari, "Comparison of polyaluminum silicate chloride and electrocoagulation process, in natural organic matter removal from surface water in Ghochan, Iran," *Journal of Water Chemistry and Technology*, vol. 33, no. 6, pp. 377–385, 2011.

[4] M. Malakootian, N. Radhakrishna, M. P. Mazandarany, and H. Hossaini, "Bacterial-aerosol emission from wastewater treatment plant," *Desalination and Water Treatment*, vol. 51, no. 22-24, pp. 4478–4488, 2013.

[5] X. Zheng, Z. Zhang, D. Yu et al., "Overview of membrane technology applications for industrial wastewater treatment in China to increase water supply," *Resources, Conservation and Recycling*, vol. 105, pp. 1–10, 2015.

[6] V. Singh, A. Tiwari, and M. Das, "Phyco-remediation of industrial waste-water and flue gases with algal-diesel engenderment from micro-algae: a review," *Fuel*, vol. 173, pp. 90–97, 2016.

[7] S. Natarajan, H. C. Bajaj, and R. J. Tayade, "Recent advances based on the synergetic effect of adsorption for removal of dyes from waste water using photocatalytic process," *Journal of Environmental Sciences*, vol. 65, pp. 201–222, 2018.

[8] E. A. Dil, M. Ghaedi, A. M. Ghaedi et al., "Modeling of quaternary dyes adsorption onto ZnO-NR-AC artificial neural network: analysis by derivative spectrophotometry," *Journal of Industrial and Engineering Chemistry*, vol. 34, pp. 186–197, 2016.

[9] A. Ayach, S. Fakhi, Z. Faiz et al., "Adsorption of methylene blue on bituminous schists from Tarfaya-Boujdour," *Chemistry International*, vol. 3, pp. 442–451, 2017.

[10] M. Abbas, M. Adil, S. Ehtisham-ul-Haque et al., "Vibrio fischeri bioluminescence inhibition assay for ecotoxicity assessment: a review," *Science of the Total Environment*, vol. 626, pp. 1295–1309, 2018.

[11] S. de Gisi, G. Lofrano, M. Grassi, and M. Notarnicola, "Characteristics and adsorption capacities of low-cost sorbents for wastewater treatment: a review," *Sustainable Materials and Technologies*, vol. 9, pp. 10–40, 2016.

[12] Y. Zhang, B. Wu, H. Xu et al., "Nanomaterials-enabled water and wastewater treatment," *NanoImpact*, vol. 3-4, pp. 22–39, 2016.

[13] M. Iqbal, M. Abbas, and A. Nazir, "Bioassays based on higher plants as excellent dosimeters for ecotoxicity monitoring: a review," *Chemistry International*, vol. 5, pp. 1–80, 2019.

[14] N. Mohammadi, H. Khani, V. K. Gupta, E. Amereh, and S. Agarwal, "Adsorption process of methyl orange dye onto mesoporous carbon material- kinetic and thermodynamic studies," *Journal of Colloid and Interface Science*, vol. 362, no. 2, pp. 457–462, 2011.

[15] M. Iqbal, "Vicia faba bioassay for environmental toxicity monitoring: a review," *Chemosphere*, vol. 144, pp. 785–802, 2016.

[16] R. Saravanan, S. Karthikeyan, V. K. Gupta, G. Sekaran, V. Narayanan, and A. Stephen, "Enhanced photocatalytic activity of ZnO/CuO nanocomposite for the degradation of textile dye on visible light illumination," *Materials Science and Engineering: C*, vol. 33, no. 1, pp. 91–98, 2013.

[17] M. Malakootian, A. Nasiri, A. Asadipour, and E. Kargar, "Facile and green synthesis of $ZnFe_2O_4$@CMC as a new magnetic nanophotocatalyst for ciprofloxacin degradation from aqueous media," *Process Safety and Environmental Protection*, vol. 129, pp. 138–151, 2019.

[18] R. Saravanan, V. K. Gupta, V. Narayanan, and A. Stephen, "Visible light degradation of textile effluent using novel catalyst ZnO/γ-Mn2O3," *Journal of the Taiwan Institute of Chemical Engineers*, vol. 45, no. 4, pp. 1910–1917, 2014.

[19] A. Kausar, M. Iqbal, A. Javed et al., "Dyes adsorption using clay and modified clay: a review," *Journal of Molecular Liquids*, vol. 256, pp. 395–407, 2018.

[20] V. Katheresan, J. Kansedo, and S. Y. Lau, "Efficiency of various recent wastewater dye removal methods: a review," *Journal of Environmental Chemical Engineering*, vol. 6, no. 4, pp. 4676–4697, 2018.

[21] A. F. S. Costa, C. D. C. Albuquerque, A. A. Salgueiro, and L. A. Sarubbo, "Color removal from industrial dyeing and laundry effluent by microbial consortium and coagulant agents," *Process Safety and Environmental Protection*, vol. 118, pp. 203–210, 2018.

[22] B. Bharathiraja, I. A. E. Selvakumari, J. Iyyappan, and S. Varjani, "Itaconic acid: an effective sorbent for removal of pollutants from dye industry effluents," *Current Opinion in Environmental Science & Health*, vol. 12, pp. 6–17, 2019.

[23] A. Saravanan, R. Jayasree, R. V. Hemavathy et al., "Phytoremediation of Cr(VI) ion contaminated soil using Black gram (*Vigna mungo*): Assessment of removal capacity," *Journal of Environmental Chemical Engineering*, vol. 7, no. 3, article 103052, 2019.

[24] L. Gan, F. Zhou, G. Owens, and Z. Chen, "Burkholderia cepacia immobilized on eucalyptus leaves used to simultaneously remove malachite green (MG) and Cr(VI)," *Colloids and Surfaces B: Biointerfaces*, vol. 172, pp. 526–531, 2018.

[25] A. A. El-Zahhar and N. S. Awwad, "Removal of malachite green dye from aqueous solutions using organically modified hydroxyapatite," *Journal of Environmental Chemical Engineering*, vol. 4, no. 1, pp. 633–638, 2016.

[26] F. Jiang, D. M. Dinh, and Y. L. Hsieh, "Adsorption and desorption of cationic malachite green dye on cellulose nanofibril aerogels," *Carbohydrate Polymers*, vol. 173, pp. 286–294, 2017.

[27] T. P. Krishna Murthy, B. S. Gowrishankar, M. N. Chandra Prabha, M. Kruthi, and R. Hari Krishna, "Studies on batch adsorptive removal of malachite green from synthetic wastewater using acid treated coffee husk: equilibrium, kinetics and thermodynamic studies," *Microchemical Journal*, vol. 146, pp. 192–201, 2019.

[28] S. Hajialigol and S. Masoum, "Optimization of biosorption potential of nano biomass derived from walnut shell for the removal of Malachite Green from liquids solution: experimental design approaches," *Journal of Molecular Liquids*, vol. 286, article 110904, 2019.

[29] S. Jeevanantham, A. Saravanan, R. V. Hemavathy, P. S. Kumar, P. R. Yaashikaa, and D. Yuvaraj, "Removal of toxic pollutants from water environment by phytoremediation: a survey on application and future prospects," *Environmental Technology & Innovation*, vol. 13, pp. 264–276, 2019.

[30] A. Saravanan, S. Karishma, S. Jeevanantham et al., "Optimization and modeling of reactive yellow adsorption by surface modified Delonix regia seed: study of nonlinear isotherm and kinetic parameters," *Surfaces and Interfaces*, vol. 20, article 100520, 2020.

[31] V. Tharaneedhar, P. Senthil Kumar, A. Saravanan, C. Ravikumar, and V. Jaikumar, "Prediction and interpretation of adsorption parameters for the sequestration of methylene blue dye from aqueous solution using microwave assisted corncob activated carbon," *Sustainable Materials and Technologies*, vol. 11, pp. 1–11, 2017.

[32] A. E. Burakov, E. V. Galunin, I. V. Burakova et al., "Adsorption of heavy metals on conventional and nanostructured materials for wastewater treatment purposes: a review," *Ecotoxicology and Environmental Safety*, vol. 148, pp. 702–712, 2018.

[33] T. N. Chikwe, R. E. Ekpo, and I. Okoye, "Competitive adsorption of organic solvents using modified and unmodified calcium bentonite clay mineral," *Chemistry International*, vol. 4, pp. 230–239, 2018.

[34] V. K. G. Suhas, P. J. M. Carrott, R. Singh, M. Chaudhary, and S. Kushwaha, "Cellulose: a review as natural, modified and activated carbon adsorbent," *Bioresource Technology*, vol. 216, pp. 1066–1076, 2016.

[35] S. Sadaf, H. N. Bhatti, S. Nausheen, and M. Amin, "Application of a novel lignocellulosic biomaterial for the removal of Direct Yellow 50 dye from aqueous solution: batch and column study," *Journal of the Taiwan Institute of Chemical Engineers*, vol. 47, pp. 160–170, 2015.

[36] R. V. Hemavathy, P. S. Kumar, K. Kanmani, and N. Jahnavi, "Adsorptive separation of Cu(II) ions from aqueous medium using thermally/chemically treated *Cassia fistula* based biochar," *Journal of Cleaner Production*, vol. 249, article 119390, 2020.

[37] A. Saravanan, S. Jeevanantham, P. Senthil Kumar, S. Varjani, P. R. Yaashikaa, and S. Karishma, "Enhanced Zn(II) ion adsorption on surface modified mixed biomass - Borassus flabellifer and Aspergillus tamarii: equilibrium, kinetics and thermodynamics study," *Industrial Crops and Products*, vol. 153, article 112613, 2020.

[38] M. M. Meimand, N. Javid, and M. Malakootian, "Adsorption of sulfur dioxide on clinoptilolite/nano iron oxide and natural clinoptilolite," *Health Scope*, vol. 8, no. 2, article e69158, 2019.

[39] F. Nekouei, S. Nekouei, I. Tyagi, and V. K. Gupta, "Kinetic, thermodynamic and isotherm studies for acid blue 129 removal from liquids using copper oxide nanoparticle-modified activated carbon as a novel adsorbent," *Journal of Molecular Liquids*, vol. 201, pp. 124–133, 2015.

[40] S. Suganya, P. Senthil Kumar, A. Saravanan, P. Sundar Rajan, and C. Ravikumar, "Computation of adsorption parameters for the removal of dye from wastewater by microwave assisted sawdust: theoretical and experimental analysis," *Environmental Toxicology and Pharmacology*, vol. 50, pp. 45–57, 2017.

[41] L. Lin, S. Tang, X. Wang, X. Sun, and A. Yu, "Adsorption of malachite green from aqueous solution by nylon microplastics: reaction mechanism and the optimum conditions by response surface methodology," *Process Safety and Environmental Protection*, vol. 140, pp. 339–347, 2020.

[42] F. Bouaziz, M. Koubaa, F. Kallel, R. E. Ghorbel, and S. E. Chaabouni, "Adsorptive removal of malachite green from aqueous solutions by almond gum: kinetic study and equilibrium isotherms," *International Journal of Biological Macromolecules*, vol. 105, Part 1, pp. 56–65, 2017.

[43] J. Wu, J. Yang, P. Feng, G. Huang, C. Xu, and B. Lin, "High-efficiency removal of dyes from wastewater by fully recycling litchi peel biochar," *Chemosphere*, vol. 246, article 125734, 2020.

[44] P. Geetha, M. S. Latha, and M. Koshy, "Biosorption of malachite green dye from aqueous solution by calcium alginate nanoparticles: equilibrium study," *Journal of Molecular Liquids*, vol. 212, pp. 723–730, 2015.

[45] S. Banerjee, G. C. Sharma, R. K. Gautam, M. C. Chattopadhyaya, S. N. Upadhyay, and Y. C. Sharma, "Removal of Malachite Green, a hazardous dye from aqueous solutions using Avena sativa (oat) hull as a potential adsorbent," *Journal of Molecular Liquids*, vol. 213, pp. 162–172, 2016.

[46] H. A. Chanzu, J. M. Onyari, and P. M. Shiundu, "Brewers' spent grain in adsorption of aqueous Congo Red and malachite Green dyes: batch and continuous flow systems," *Journal of Hazardous Materials*, vol. 380, p. 120897, 2019.

[47] E. Mkrtchyan, A. Burakov, and I. Burakova, "The adsorption of malachite green on graphene nanocomposites: a study on kinetics under dynamic conditions," *Materials Today: Proceedings*, vol. 11, pp. 404–409, 2019.

[48] P. Saha, S. Chowdhury, S. Gupta, and I. Kumar, "Insight into adsorption equilibrium, kinetics and thermodynamics of Malachite Green onto clayey soil of Indian origin," *Chemical Engineering Journal*, vol. 165, no. 3, pp. 874–882, 2010.

[49] Q. Baocheng, J. Zhou, X. Xiang, C. Zheng, H. Zhao, and X. Zhou, "Adsorption behavior of Azo Dye C. I. Acid Red 14 in aqueous solution on surface soils," *Journal of Environmental Sciences*, vol. 20, no. 6, pp. 704–709, 2008.

[50] J.-B. Tarkwa, E. Acayanka, B. Jiang et al., "Highly efficient degradation of azo dye Orange G using laterite soil as catalyst under irradiation of non-thermal plasma," *Applied Catalysis B: Environmental*, vol. 246, pp. 211–220, 2019.

[51] W. Astuti, A. Chafidz, E. T. Wahyuni, A. Prasetya, I. M. Bendiyasa, and A. E. Abasaeed, "Methyl violet dye removal using coal fly ash (CFA) as a dual sites adsorbent," *Journal of Environmental Chemical Engineering*, vol. 7, no. 5, article 103262, 2019.

[52] A. Saravanan, T. R. Sundararaman, S. Jeevanantham, S. Karishma, P. S. Kumar, and P. R. Yaashikaa, "Effective adsorption of Cu(II) ions on sustainable adsorbent derived from mixed biomass (Aspergillus campestris and agro waste): optimization, isotherm and kinetics study," *Groundwater for Sustainable Development*, vol. 11, article 100460, 2020.

[53] R. Jothirani, P. S. Kumar, A. Saravanan, A. S. Narayan, and A. Dutta, "Ultrasonic modified corn pith for the sequestration of dye from aqueous solution," *Journal of Industrial Engineering Chemistry*, vol. 39, pp. 162–175, 2016.

[54] S. Lagergren, "About the theory of so-called adsorption of soluble substances," *Kungliga Svenska Vetenskapsakademiens Handlingar*, vol. 24, pp. 1–39, 1898.

[55] Y. S. Ho and G. McKay, "Pseudo-second order model for sorption processes," *Process Biochemistry*, vol. 34, no. 5, pp. 451–465, 1999.

[56] M. J. D. Low, "Kinetics of chemisorption of gases on solids," *Chemical Reviews*, vol. 60, no. 3, pp. 267–312, 1960.

[57] H. N. Bhatti, A. Jabeen, M. Iqbal, S. Noreen, and Z. Naseem, "Adsorptive behavior of rice bran-based composites for malachite green dye: isotherm, kinetic and thermodynamic studies," *Journal of Molecular Liquids*, vol. 237, pp. 322–333, 2017.

[58] I. Langmuir, "The adsorption of gases on plane surfaces of glass, mica and platinum," *Journal of the American Chemical Society*, vol. 40, no. 9, pp. 1361–1403, 1918.

[59] H. M. F. Freundlich, "Over the adsorption in solution," *The Journal of Physical Chemistry*, vol. 57, pp. 385–470, 1906.

[60] A. Khan, R. Ataullah, and A. Al-Haddad, "Equilibrium adsorption studies of some aromatic pollutants from dilute aqueous solutions on activated carbon at different temperatures," *Journal of Colloid and Interface Science*, vol. 194, no. 1, pp. 154–165, 1997.

[61] L. Jossens, J. M. Prausnitz, W. Fritz, E. U. Schlünder, and A. L. Myers, "Thermodynamics of multi-solute adsorption from dilute aqueous solutions," *Chemical Engineering Science*, vol. 33, no. 8, pp. 1097–1106, 1978.

[62] S. Chowdhury and P. Das, "Mechanistic, kinetic, and thermodynamic evaluation of adsorption of hazardous malachite green onto conch shell powder," *Separation Science and Technology*, vol. 46, no. 12, pp. 1966–1976, 2011.

[63] W. Qu, T. Yuan, G. Yin, S. Xu, Q. Zhang, and H. Su, "Effect of properties of activated carbon on malachite green adsorption," *Fuel*, vol. 249, pp. 45–53, 2019.

[64] A. S. Sartape, A. M. Mandhare, V. V. Jadhav, P. D. Raut, M. A. Anuse, and S. S. Kolekar, "Removal of malachite green dye from aqueous solution with adsorption technique using Limonia acidissima (wood apple) shell as low cost adsorbent," *Arabian Journal of Chemistry*, vol. 10, pp. S3229–S3238, 2017.

[65] I. A. Rahman, B. Saad, S. Shaidan, and E. Syarizal, "Adsorption characteristics of malachite green on activated carbon derived from rice husks produced by chemical-thermal process," *Bioresource Technology*, vol. 96, no. 14, pp. 1578–1583, 2005.

[66] V. K. Garg, R. Kumar, and R. Gupta, "Removal of malachite green dye from aqueous solution by adsorption using agro-industry waste: a case study of Prosopis cineraria," *Dyes and Pigments*, vol. 62, no. 1, pp. 1–10, 2004.

[67] B. H. Hameed and M. I. El-Khaiary, "Malachite green adsorption by rattan sawdust: isotherm, kinetic and mechanism modeling," *Journal of Hazardous Materials*, vol. 159, no. 2-3, pp. 574–579, 2008.

[68] W. Zou, K. Li, H. Bai, X. Shi, and R. Han, "Enhanced cationic dyes removal from aqueous solution by oxalic acid modified rice husk," *Journal of Chemical & Engineering Data*, vol. 56, no. 5, pp. 1882–1891, 2011.

[69] H. H. Hammud, A. Shmait, and N. Hourani, "Removal of malachite green from water using hydrothermally carbonized pine needles," *RSC Advances*, vol. 5, no. 11, pp. 7909–7920, 2015.

[70] S. Nethaji, A. Sivasamy, G. Thennarasu, and S. Saravanan, "Adsorption of Malachite Green dye onto activated carbon derived from Borassus aethiopum flower biomass," *Journal of Hazardous Materials*, vol. 181, no. 1-3, pp. 271–280, 2010.

[71] A. Mohammadi, H. Daemi, and M. Barikani, "Fast removal of malachite green dye using novel superparamagnetic sodium alginate-coated Fe_3O_4 nanoparticles," *International Journal of Biological Macromolecules*, vol. 69, pp. 447–455, 2014.

[72] T. A. Khan, R. Rahman, I. Ali, E. A. Khan, and A. A. Mukhlif, "Removal of malachite green from aqueous solution using waste pea shells as low-cost adsorbent – adsorption isotherms and dynamics," *Environmental Toxicology and Chemistry*, vol. 96, no. 4, pp. 569–578, 2014.

[73] A. Mittal, L. Krishnan, and V. K. Gupta, "Removal and recovery of malachite green from wastewater using an agricultural waste material, de-oiled soya," *Separation and Purification Technology*, vol. 43, no. 2, pp. 125–133, 2005.

[74] T. K. Arumugam, P. Krishnamoorthy, N. R. Rajagopalan, S. Nanthini, and D. Vasudevan, "Removal of malachite green from aqueous solutions using a modified chitosan composite," *International Journal of Biological Macromolecules*, vol. 128, pp. 655–664, 2019.